



## A Cationic Copolymer as a Cocatalyst for a Peroxidase-Mimicking Heme-DNAzyme

Journal:	<i>Biomaterials Science</i>
Manuscript ID	BM-ART-06-2021-000949.R2
Article Type:	Paper
Date Submitted by the Author:	27-Jul-2021
Complete List of Authors:	Araki, Haruka; University of Tsukuba, Chemistry Hagiwara, Shota; University of Tsukuba, Chemistry Shinomiya, Ryosuke; University of Tsukuba, Chemistry Momotake, Atsuya; University of Tsukuba, Chemistry Kotani, Hiroaki; University of Tsukuba, Department of Chemistry Kojima, Takahiko; University of Tsukuba, Department of Chemistry Ochiai, Takuro; Tokyo Institute of Technology, Life Science and Technology Shimada, Naohiko; Tokyo Institute of Technology, Department of Life Science and Technology Maruyama, Atsushi; Tokyo Institute of Technology, Life Science and Technology Yamamoto, Yasuhiko; University of Tsukuba, Chemistry

## ARTICLE

## A cationic copolymer as a cocatalyst for a peroxidase-mimicking heme-DNAzyme

Received 00th January 20xx,  
Accepted 00th January 20xx

Haruka Araki,<sup>a</sup> Shota Hagiwara,<sup>a</sup> Ryosuke Shinomiya,<sup>a</sup> Atsuya Momotake,<sup>a</sup> Hiroaki Kotani,<sup>a</sup> Takahiko Kojima,<sup>a</sup> Takuro Ochiai,<sup>b</sup> Naohiko Shimada,<sup>b</sup> Atsushi Maruyama,<sup>b</sup> and Yasuhiko Yamamoto<sup>\*a,c</sup>

DOI: 10.1039/x0xx00000x

Heme binds to a parallel-stranded G-quadruplex DNA to form a peroxidase-mimicking heme-DNAzyme. An interpolyelectrolyte complex between the heme-DNAzyme and a cationic copolymer possessing protonated amino groups was characterized and the peroxidase activity of the complex was evaluated to elucidate the effect of the polymer on the catalytic activity of the heme-DNAzyme. We found that the catalytic activity of the heme-DNAzyme is enhanced through the formation of the interpolyelectrolyte complex due to the general acid catalysis of protonated amino groups of the polymer, enhancing the formation of the iron(IV)oxo porphyrin  $\pi$ -cation radical intermediate known as Compound I. This finding indicates that the polymer with protonated amino groups can act as a cocatalyst for the heme-DNAzyme in the oxidation catalysis. We also found that the enhancement of the activity of the heme-DNAzyme by the polymer depends on the local heme environment such as the negative charge density in the proximity of the heme and substrate accessibility to the heme. These findings provide novel insights as to molecular design of the heme-DNAzyme for enhancing its catalytic activity.

### Introduction

Heme (heme( $\text{Fe}^{2+}$ ) or hemin (heme( $\text{Fe}^{3+}$ ))) (Fig. 1A)) is a ubiquitous and abundant cellular cofactor responsible for a variety of metabolic functions.<sup>1</sup> Heme is incorporated into various apoproteins to form a series of hemoproteins that exhibit diverse functions, and the functional diversity of heme in hemoproteins arises through its interaction with various apoproteins. Sen and co-workers<sup>2-9</sup> demonstrated that heme( $\text{Fe}^{3+}$ ) binds to non-canonical G-quadruplex DNAs to form complexes that exhibit peroxidase and peroxygenase activities. This finding triggered exploration of the biological versatility of heme as the prosthetic group of DNAzymes, and interaction between heme and G-quadruplex DNAs has been investigated extensively to elucidate the structure-function relationship of DNAzyme possessing heme (heme-DNAzyme) and also to improve the catalytic activity of the heme-DNAzyme.<sup>10-35</sup>

The peroxidase activity of heme-DNAzyme is elicited through a reaction mechanism similar to those of peroxidases such as horseradish peroxidase (HRP).<sup>18</sup> The catalytic cycle of the heme-DNAzyme involves an iron(IV)oxo porphyrin  $\pi$ -cation radical intermediate known as Compound I formed through heterolytic O-O bond cleavage of an Fe-bound hydroperoxy ligand (Fe-

OOH) in Compound 0 (Scheme 1).<sup>36-41</sup> In the case of HRP, the electron-donating effect of the proximal His (His170), and the concerted action of the distal His (His42) and a nearby positively-charged amino acid side chain (Arg38), as general base and acid catalysts, respectively, play important roles to promote the formation of Compound I (Scheme 1B).<sup>36,37</sup>

Heme binds to a unique structural motif known as the G-quartet, which is formed through cyclic and coplanar association of four guanine bases (Fig. 1B).<sup>42</sup> In a complex between heme and a parallel-stranded tetrameric G-quadruplex DNA of a hexanucleotide d(TTAGGG) (6mer) (heme-6mer complex: Fig. 1C), heme binds selectively to the 3'-terminal G-quartet of the DNA, and a water molecule sandwiched between the heme and G-quartet planes ( $\text{AxH}_2\text{O}$ : Fig. 1D) and an exogenous ligand are coordinated to the heme Fe atom as axial ligands.<sup>14</sup> Moreover,  $\text{AxH}_2\text{O}$  possibly forms hydrogen bonds with carbonyl oxygen atoms of guanine bases of the nearby G-quartet (Fig. 1D) and, due to such a unique chemical environment of  $\text{AxH}_2\text{O}$ , the polarization of  $\text{AxH}_2\text{O}$  is thought to be considerably greater than that of an ordinary  $\text{H}_2\text{O}$  molecule. In fact, the heme-DNAzyme exhibits various spectroscopic and functional properties remarkably similar to those of myoglobin (Mb),<sup>11,13,15,16</sup> supporting that the electronic nature of  $\text{AxH}_2\text{O}$  in the complex is similar to that of the axial His in Mb, although the donor strength of  $\text{AxH}_2\text{O}$  is weaker than that of the His<sup>16</sup>. Consequently,  $\text{AxH}_2\text{O}$  in the heme-DNAzyme possibly plays an important electronic role similar to that of His170 in HRP. In addition, the adenine base adjacent to the heme in the heme-DNAzyme was found to act as a general base catalyst that promotes the formation of Compound 0, like the His42 side chain in HRP (Scheme 1B).<sup>17,19,24</sup>

<sup>a</sup> Department of Chemistry, University of Tsukuba, Tsukuba 305-8571, Japan

<sup>b</sup> School of Life Science and Technology, Tokyo Institute of Technology, Yokohama 226-8501, Japan

<sup>c</sup> Tsukuba Research Center for Energy Materials Science (TREMS), University of Tsukuba, Tsukuba 305-8571, Japan

H. A. and S. H. contributed equally to this work.

† Electronic Supplementary Information (ESI) available: [Figs. S1 – S9]. See DOI: 10.1039/x0xx00000x

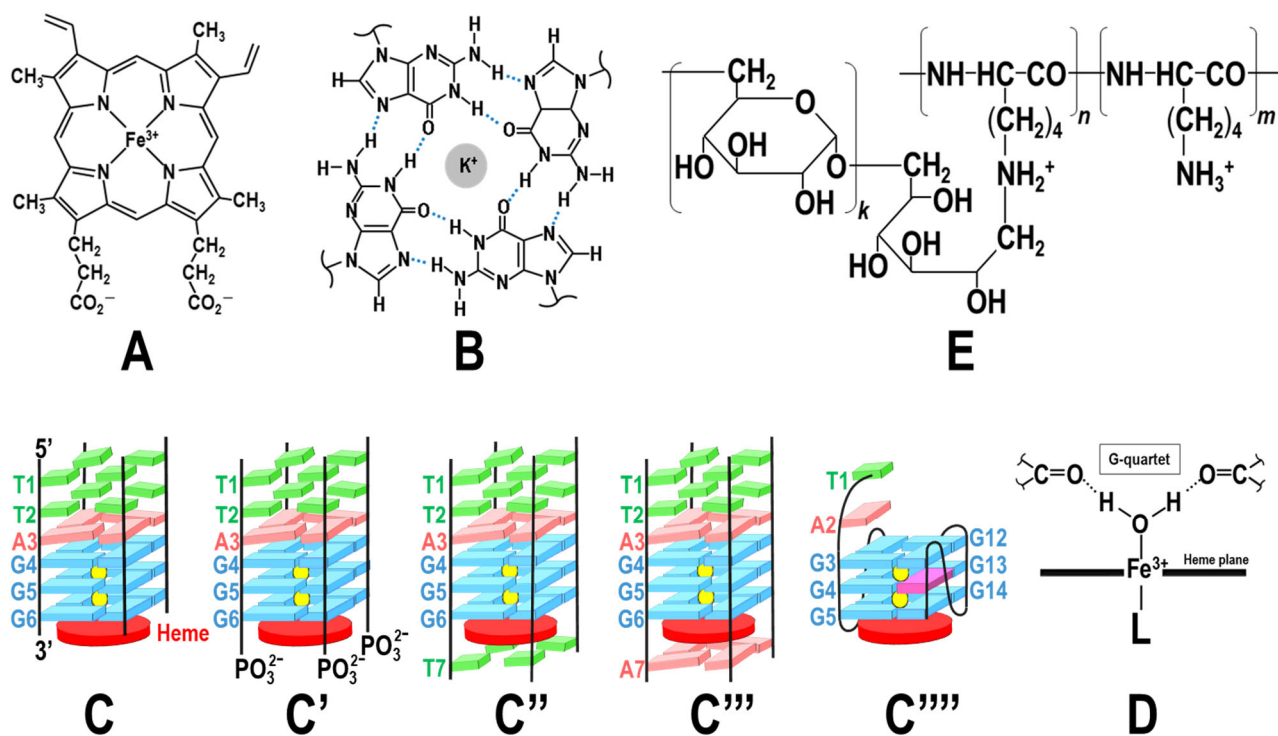
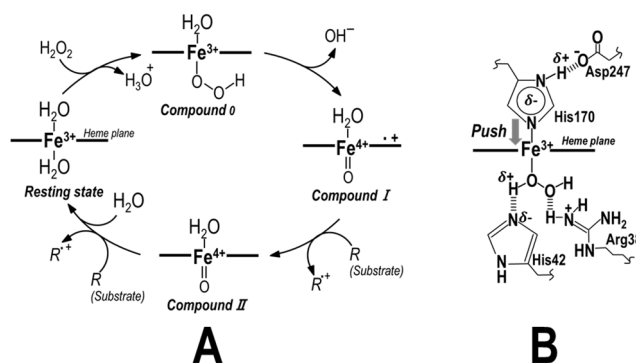


**Fig. 1** Molecular structures of heme( $\text{Fe}^{3+}$ ) (A) and the G-quartet (B), schematic representations of complexes between heme and parallel G-quadruplex DNAs formed from d(TTAGGG) (6mer), d(TTAGGGp) (6mer/p), d(TTAGGGT) (6mer/T), d(TTAGGGA) (6mer/A), and non-standard base inosine(I)-containing sequence d(TAGGGTGGGTTGGGTGIG) (18mer), i.e., the heme-6mer<sup>11</sup> (C), heme-6mer/p (C'), heme-6mer/T<sup>15</sup> (C''), heme-6mer/A<sup>19</sup> (C'''), and heme-18mer<sup>17</sup> complexes (C'''). the heme( $\text{Fe}^{3+}$ ) coordination structure of the complex (D)<sup>14</sup>, and chemical structure of a cationic copolymer, PLL-g-Dex (E).

Various strategies have been devised to improve the catalytic activity of heme-DNAzymes. Modification of the DNA scaffold through alteration of the constituent DNA sequence<sup>23-26</sup> and the addition of ammonium ion<sup>27-30</sup> and biogenic polyamines<sup>31</sup> such as spermine, spermidine, and putrescine have been reported to be successful for enhancing the activity of heme-DNAzymes. The formation of interpolyelectrolyte complexes of DNAs with cationic polymers has been used extensively to modulate the structural and functional properties of DNAs for various pharmaceutical and biomedical applications.<sup>43-50</sup> Sato et al.<sup>50</sup> demonstrated that a cationic copolymer composed of poly(L-lysine) and dextran, as main and hydrophilic graft chains, respectively (PLL-g-Dex (Fig. 1E)), enhances the peroxidase activity of a heme-DNAzyme. Upon the binding of PLL-g-Dex to G-quadruplex-forming DNA sequences, the parallel G-quadruplex structure is selectively stabilized over other ones such as antiparallel and (3+1) hybrid ones, and hence the enhancement of the activity of heme-DNAzymes by PLL-g-Dex is explained in terms of the predominance of parallel G-quadruplex DNAs, in the presence of the polymer, which bind heme( $\text{Fe}^{3+}$ ) with high affinity to form complexes that exhibit high peroxidase activity.<sup>47</sup> Since PLL-g-Dex possesses positively-charged amino groups capable of being general acid catalysts, like the Arg38 side chain in HRP (Scheme 1B) and forms a stable interpolyelectrolyte complex with DNA,<sup>43</sup> the polymer is expected to serve as a cocatalyst for the heme-DNAzyme.

In this study, we examined the use of PLL-g-Dex as a cocatalyst for the heme-DNAzyme not only to develop a methodology aimed at further enhancement of its catalytic activity, but also to gain a deeper understanding of the structure-function relationship of the heme-DNAzyme. In addition to a heme-6mer complex, all parallel-stranded tetrameric G-quadruplex DNAs formed from d(TTAGGGp) (where p represents an additional phosphate group bonded to the 3'-terminal of the sequence) (6mer/p), d(TTAGGGT) (6mer/T), d(TTAGGGA) (6mer/A), and non-standard base inosine(I)-containing sequence d(TAGGGTGGGTTGGGTGIG) (18mer) were used to prepare complexes, i.e., the heme-6mer/p, heme-6mer/T, heme-6mer/A, and heme-18mer complexes, respectively (Figs. 1C-C'''), and the catalytic activities of the complexes in the presence of PLL-g-Dex were evaluated to elucidate the impact of a local environment around the heme attached to the 3'-terminal G-quartet of a G-quadruplex DNA. The study revealed that PLL-g-Dex can be a cocatalyst for the heme-DNAzyme. The enhancement of the catalytic activity of the complex bearing PLL-g-Dex was found to vary with the DNA sequence, indicating that the enhancement of the activity of the heme-DNAzyme by the polymer depends on the local heme environment such as the negative charge density in the proximity of the heme and substrate accessibility to the heme.

## MATERIALS AND METHODS



**Scheme 1.** Catalytic cycle of the heme-DNAzyme<sup>18</sup> (A) and schematic representation of the active site of horseradish peroxidase (HRP)<sup>40</sup> (B). In (B), amino acid residues involved in the catalytic cycle<sup>37</sup> are shown.

### Sample preparation

DNA sequences, d(TTAGGG), d(TTAGGGp; where p represents an additional phosphate group bound to the 3'-terminal of the sequence), d(TTAGGGT), d(TTAGGGA), and d(TAGGGTG GTTGGGTGIG), purified with a C-18 Sep-Pak cartridge were purchased from Tsukuba Oligo Service Co. The oligonucleotides were further purified by ethanol precipitation and then desalted with Microcon YM-3 (Millipore, Bedford, MA). The concentration of each oligonucleotide was determined spectrophotometrically using the absorbance at 260 nm (molar extinction coefficients  $\epsilon_{260} = 6.89 \times 10^4$ ,  $6.89 \times 10^4$ ,  $7.81 \times 10^4$ ,  $8.43 \times 10^4$ , and  $2.01 \times 10^5$  cm<sup>-1</sup> M<sup>-1</sup> for d(TTAGGG), d(TTAGGGp), d(TTAGGGT), d(TTAGGGA), and d(TAGGGT GGGTGGGTGIG), respectively). Heme(Fe<sup>3+</sup>) was purchased from Sigma-Aldrich Co. Preparation of the heme(Fe<sup>3+</sup>)-DNA complexes was carried out by mixing 5 - 20  $\mu$ M heme(Fe<sup>3+</sup>) and 10 - 40  $\mu$ M G-quadruplex DNA as described previously.<sup>14</sup> Horseradish peroxidase (HRP) was purchased as a lyophilized powder from Sigma-Aldrich Co. and used without further purification.

A cationic polymer (PLL-g-Dex) was synthesized from poly(L-lysine hydrobromide) (PLL•HBr, Mw =  $8.0 \times 10^3$ ) and dextran (Mw(averaged) =  $1.05 \times 10^4$ ),<sup>50</sup> purchased from Sigma-Aldrich (St. Louis, MO, USA) and Funakoshi Co. (Tokyo, Japan), respectively. Dextran was conjugated to amino groups of PLL by means of the reductive amination reaction. The copolymer was purified by ion exchange followed by dialysis against water, and then lyophilized. The dextran content of PLL-g-Dex used in this study was 90 wt%. The average numbers of lysine repeating units and dextran grafts of the copolymer were 62 and 8.7, respectively. The concentration of PLL-g-Dex, relative to that of DNA, is expressed in terms of the ratio between the numbers of protonated amino groups in the polymer and PO<sub>4</sub><sup>-</sup> groups in the phosphodiester bonds of the DNA (*N/P*). The 3'-terminal phosphate group of 6mer/p at neutral pH exists as monoanionic and dianion states, which are in equilibrium with a pK<sub>a</sub> of ~6.0~7.0,<sup>51</sup> and the *N/P* of the 6mer/p system was calculated with the assumption that the 3'-terminal phosphate group of the DNA exists predominantly as a monoanion. In order

to evaluate the effects of the dextran moiety of PLL-g-Dex on the catalytic activity of the heme-DNAzyme, cocatalytic activity of the dextran used to prepare PLL-g-Dex was also examined.

### UV-vis absorption and NMR spectroscopies

UV-Vis absorption spectra were recorded at 25 °C with a Jasco V750 spectrophotometer using 50 mM potassium phosphate buffer, pH 6.80, containing 300 mM KCl as a solvent. (d(TTAGGG))<sub>4</sub>, (d(TTAGGGp))<sub>4</sub>, (d(TTAGGGA))<sub>4</sub>, and (d(TTAGGGT))<sub>4</sub> in 50 mM potassium phosphate buffer, pH 6.80, were heat-denatured at 90 °C for 5 min., followed by cooling to 25 °C. <sup>1</sup>H NMR spectra were recorded on a Bruker AVANCE 600 spectrometer (Bruker, USA) operating at a <sup>1</sup>H frequency of 600 MHz. Typical spectra were obtained with a 20 ppm spectral width, 32 k data points, a 2 s relaxation delay, and 64 transients at 25 °C. The signal-to-noise ratio of the spectra was improved by apodization, which introduced 0.3 Hz line-broadening. The chemical shifts of <sup>1</sup>H NMR spectra are referred to external 2,2-dimethyl-2-silapentane-5-sulfonate.

### Amplex Red oxidation kinetics

A chromogenic substrate, 10-acetyl-3,7-dihydroxyphenoxazine (Amplex Red), was purchased from Sigma-Aldrich, and the reaction was monitored by following the appearance of the oxidized product, 7-hydroxyphenoxazin-3-one (Resorufin), which absorbs light at ~570 nm. Kinetic studies were performed on a Jasco V 750 spectrometer. Amplex Red was dissolved in dimethylformamide to prepare a 10 mM stock solution. Heme(Fe<sup>3+</sup>) and then Amplex Red were added to 0.5  $\mu$ M and 50  $\mu$ M, respectively, to 20  $\mu$ M G-quadruplex DNA in 50 mM potassium phosphate buffer, pH 6.80. To initiate the oxidation reactions, 200  $\mu$ M hydrogen peroxide (H<sub>2</sub>O<sub>2</sub>) was added to the solution mixture. The initial slope (*R*<sub>0</sub>) of the time evolution of 570-nm absorbance due to Resorufin was used as an index for the peroxidase activities of the complexes. In order to evaluate deuterium kinetic isotope effects, the peroxidase assay of the heme(Fe<sup>3+</sup>)-6mer complex in ~100% <sup>2</sup>H<sub>2</sub>O was also performed.

In addition, the turnover frequencies (TOFs) for Amplex Red oxidation by the heme(Fe<sup>3+</sup>)-6mer complex in the absence and presence of PLL-g-Dex were determined and analyzed in order to elucidate the effects of the polymer on the catalytic activity of the heme-DNAzyme. The TOFs obtained for the heme-DNAzyme were also compared with that of HRP measured under the identical reaction conditions except the concentration of the catalyst, [HRP] = 1 nM.

### Electron spin resonance (ESR) spectroscopy

ESR spectra were recorded on a Bruker BioSpin X-band spectrometer (EMXPlus9.5/2.7 (Bruker, USA)) with a liquid helium transfer system operating at 9.394 GHz under nonsaturating microwave power conditions (4.0 mW). The magnitude of the modulation was chosen to optimize the resolution and the signal-to-noise (*S/N*) ratio of the observed spectrum (modulation amplitude, 5–20 G; modulation frequency, 100 kHz).

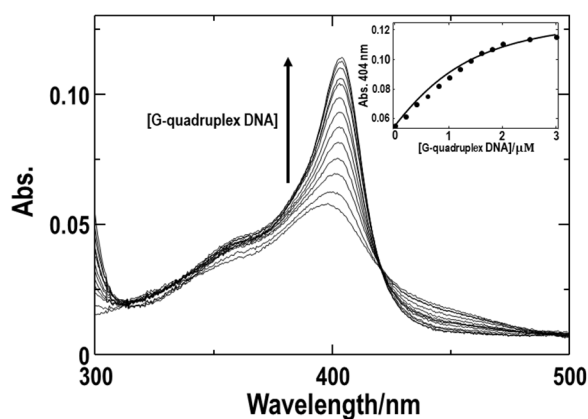


**Fig. 2** Soret absorption, 300–500 nm, of a parallel-stranded tetrameric G-quadruplex DNA (6mer/p), 0–3  $\mu\text{M}$ , titrated against 1  $\mu\text{M}$  heme( $\text{Fe}^{3+}$ ) in 300 mM KCl and 50 mM potassium phosphate buffer, pH 6.80, together with 0.08 w/v% Triton X-100 and 0.5 v/v% dimethyl sulfoxide, at 25  $^{\circ}\text{C}$ . A plot of the 404-nm absorbance against 6mer/p concentration is shown in the inset. A heme binding constant ( $K_a$ ) of  $1.7 \pm 0.4 \mu\text{M}^{-1}$  was obtained for the heme( $\text{Fe}^{3+}$ )-6mer/p complex.

For ESR samples of heme-DNA complexes, 0.1 mM heme and 0.1 mM G-quadruplex DNA were mixed in 50 mM potassium phosphate buffer, pH 6.80, and 300 mM KCl, and then 15 mM  $\text{H}_2\text{O}_2$  was added. The mixed solution was immediately frozen for the measurement at 5 K under a He atmosphere.

## RESULTS

### Heme binding affinity

The formation of parallel-stranded tetrameric G-quadruplex DNAs, i.e., 6mer, 6mer/p, 6mer/A, and 6mer/T, was confirmed by the observation of negative and positive Cotton effects at  $\sim 240$  and  $\sim 260$  nm, respectively, in their CD spectra, which were characteristic of parallel G-quadruplexes<sup>52</sup> (Fig. S1). Interaction of heme( $\text{Fe}^{3+}$ ) with the G-quadruplex DNAs was characterized using absorption spectra. Upon addition of various amounts of 6mer/p, the Soret band of 10  $\mu\text{M}$  heme( $\text{Fe}^{3+}$ ) at pH 6.80 and 25  $^{\circ}\text{C}$  exhibited a bathochromic shift showing clear isosbestic point at 420 nm in the range of 300–500 nm (Fig. 2), indicating that heme( $\text{Fe}^{3+}$ ) binds selectively to 6mer/p to form a 1:1 heme( $\text{Fe}^{3+}$ )-6mer/p complex. The absorbance change observed at 404 nm was fitted with the theoretical equation for 1:1 complexation, as described by Wang et al.,<sup>53</sup> and the binding constant ( $K_a$ ) was determined to be  $1.7 \pm 0.4 \mu\text{M}^{-1}$  (Fig. 2). The  $K_a$  determined for the heme( $\text{Fe}^{3+}$ )-6mer/p complex is compared with those previously reported for the other ones in Table 1. The  $K_a$  of  $6.5 \pm 0.7 \mu\text{M}^{-1}$  determined for the heme( $\text{Fe}^{3+}$ )-6mer complex (Fig. S2) was smaller by a factor of  $\sim 1/2.5$  compared with the value previously reported<sup>16</sup>. Considering that the range of the concentration ratio, i.e., [G-quadruplex DNA]/[heme( $\text{Fe}^{3+}$ )], used for the present measurements was larger than that used for the previous ones<sup>16</sup>, together with the better data fitting, hereafter the value determined in this study is used for the  $K_a$  of the complex.

### Interaction of a CO adduct of the heme( $\text{Fe}^{2+}$ )-6mer complex with PLL-g-Dex

The effect of PLL-g-Dex on the molecular structure of a CO adduct of the low-spin heme( $\text{Fe}^{2+}$ )-6mer complex was characterized by  $^1\text{H}$  NMR (Fig. 3). In the NMR spectrum of the heme( $\text{Fe}^{2+}$ )-6mer complex (Fig. 3B),  $\text{G4}_\text{C}$ - $\text{G6}_\text{C}$  imino, where subscript “C” represents signals due to the complex, and  $\text{A}_\text{X}\text{H}_2\text{O}$  pr and  $\text{A}_\text{X}\text{H}_2\text{O}$  signals were resolved in the downfield- and upfield-shifted portions, respectively, and  $\text{G6}_\text{C}$  and  $\text{A}_\text{X}\text{H}_2\text{O}$  signals were observed as  $\sim 1:1$  doublet peaks due to the presence of the two different heme orientations differing by  $180^\circ$  rotation about the pseudo- $\text{C}_2$  axis passing through the *meso* 5-H and 15-H hydrogens, with respect to the DNA (Fig. S3),<sup>11,13</sup> similar to the “heme orientational disorder” well-known as a common structural feature of *b*-type hemoproteins<sup>54,55</sup>. In addition, two sets of heme *meso* proton signals due to the heme orientational disorder were observed in the shift range of 9.0–9.4 ppm. With increasing polymer concentration, the resolved signals broadened, and peaks x-z emerged (Figs. 3B-B’). It has been shown that a 6mer dimerizes through intermolecular end-to-end stacking of the 3'-terminal G-quartets, i.e., G6 G-quartets (Fig. S4).<sup>56</sup> The shifts of peaks x-z were identical to those of the G4-G6 proton signals of the 6mer dimer ( $\text{G4}_\text{D}$ - $\text{G6}_\text{D}$ ) (Figs. 3A', B', and B’), allowing the assignments of peaks x, y, and z to  $\text{G4}_\text{D}$ ,  $\text{G5}_\text{D}$ , and  $\text{G6}_\text{D}$ , respectively. The spectral pattern of the resolved  $\text{G4}_\text{C}$ - $\text{G6}_\text{C}$  imino, heme *meso*, and  $\text{A}_\text{X}\text{H}_2\text{O}$  proton signals in the spectrum of a CO adduct of the heme( $\text{Fe}^{2+}$ )-6mer/p complex (Fig. 3C) is similar to that of the heme( $\text{Fe}^{2+}$ )-6mer one (Fig. 3B), indicating that heme binds selectively to the 3'-terminal G-quartet of 6mer/p. In addition, the  $\text{A}_\text{X}\text{H}_2\text{O}$  proton signal in the spectrum of the heme( $\text{Fe}^{2+}$ )-6mer/p complex was observed as a single peak, although  $\text{G6}_\text{C}$  and heme *meso* proton signals exhibited  $\sim 1:1$  splitting due to the heme orientational disorder (Fig. 3C).

### Redox potential of Amplex Red

The redox potential of Amplex Red in a buffer solution at pH 6.80 was determined by electrochemical measurements (Fig. S5). The cyclic voltammetry trace of Amplex Red in the aqueous solution exhibited an irreversible oxidation wave at 0.95 V (vs. SCE) (Fig. S5). The determined oxidation potential was higher by 0.23 V relative to the value determined for Amplex Red in acetonitrile, i.e., 0.72 V (vs. SCE).<sup>57</sup> The value of 0.88 V (vs. SCE) was determined for the oxidation potential of Amplex Red in the presence of PLL-g-Dex at  $N/P = 3.6$ . Thus, the presence of the polymer with protonated amino groups does not affect the oxidation potential of the substrate.

### Peroxidase assay of the heme( $\text{Fe}^{3+}$ )-DNA complex

The peroxidase activities of the heme-DNA complexes were analyzed on the basis of kinetic analysis of oxidation of Amplex Red to afford Resorufin showing absorption at 570 nm. An initial rate ( $R_0$ ) of the reaction was determined using the initial slope of time course of the absorbance at 570 nm. The  $R_0$  of  $0.61 \pm 0.1 \mu\text{M min}^{-1}$  obtained for the heme( $\text{Fe}^{3+}$ )-6mer/p complex (Fig. 4A) was comparable to those of the heme( $\text{Fe}^{3+}$ )-6mer and

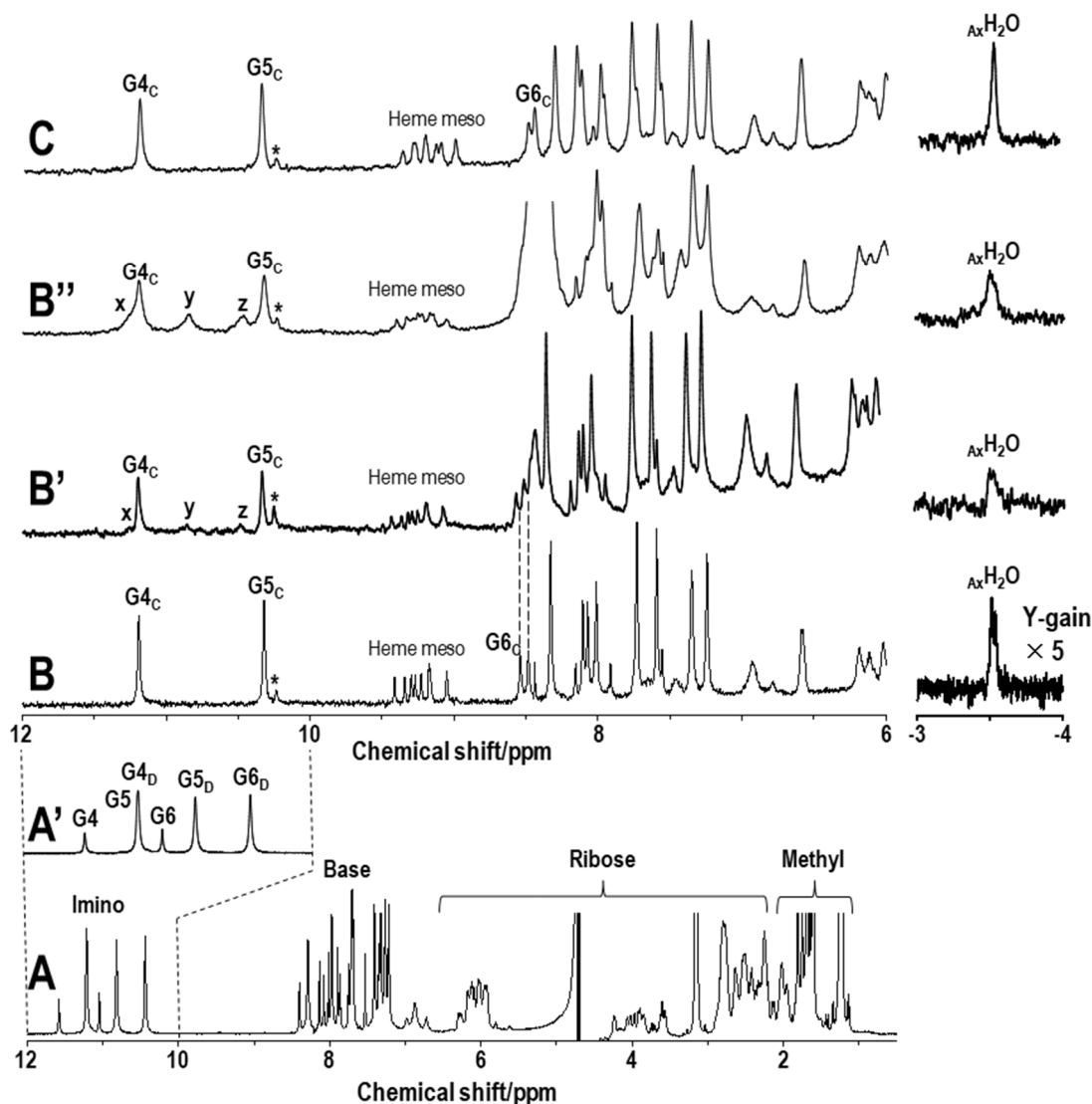


**Fig. 3** 600 MHz  $^1\text{H}$  NMR spectra of 6mer (A) and CO adducts of the heme( $\text{Fe}^{2+}$ )-6mer complex in the absence (B) and presence of PLL-*g*-Dex at  $N/P = 0.45$  ( $B'$ ) and  $N/P = 3.75$  ( $B''$ ), and the heme( $\text{Fe}^{2+}$ )-6mer/p one (C) in 90%  $^1\text{H}_2\text{O}/10\%$   $^2\text{H}_2\text{O}$ , 50 mM KCl, 50 mM potassium phosphate buffer at pH 6.80 and 25  $^\circ\text{C}$ . The chemical shift range, 10–12 ppm, of trace A is expanded in trace A'. Assignments of guanine imino, heme *meso*, and axial  $\text{H}_2\text{O}$  ( $_{\text{ax}}\text{H}_2\text{O}$ ) proton signals are indicated with the spectra.  $G_n$ , where  $n$  is the residue number, represents guanine imino proton signals, and the signals due to 6mer dimer (Fig. S4) the heme-DNA complex are indicated by subscripts D and C, respectively. Peaks  $x$ ,  $y$ , and  $z$  in traces  $B'$  and  $B''$  correspond to  $G_{4D}$ ,  $G_{5D}$ , and  $G_{6D}$ , respectively. Peaks due to impurities are indicated by  $*$ .

heme( $\text{Fe}^{3+}$ )-6mer/T complexes, i.e.,  $0.94 \pm 0.1$  and  $0.50 \pm 0.05$   $\mu\text{M min}^{-1}$ , respectively, and the value was smaller by a factor of  $\sim 1/7$  relative to that of the heme( $\text{Fe}^{3+}$ )-6mer/A counterpart, i.e.,  $4.52 \pm 0.45$   $\mu\text{M min}^{-1}$  (Table 1). In addition, the value of  $0.54 \pm 0.1$   $\mu\text{M min}^{-1}$  was obtained for the  $R_0$  of the heme( $\text{Fe}^{3+}$ )-6mer/p complex in  $\sim 100\%$   $^2\text{H}_2\text{O}$  (Table 1), indicating that the deuterium kinetic isotope effect (KIE ( $= R_0(^1\text{H})/R_0(^2\text{H})$ )) is 1.7.

Peroxidase assay of the heme( $\text{Fe}^{3+}$ )-6mer and heme( $\text{Fe}^{3+}$ )-6mer/p complexes in the presence of PLL-*g*-Dex in the  $N/P$  range of 0–7 was performed (Fig. 5). The activities of the two complexes increased with increasing the  $N/P$  and almost reached plateaus at  $N/P > 3.6$ . At  $N/P = 3.6$ , the molar ratio between PLL-*g*-Dex and the heme-DNAzyme is  $\sim 2:1$ , and the result in Fig. 5

indicated that the local heme environment in the interpolyelectrolyte complex formed at  $N/P = 3.6$  is not largely affected by the further addition of the polymer. Peroxidase assay of the other heme( $\text{Fe}^{3+}$ )-DNA complexes in the presence of PLL-*g*-Dex at  $N/P = 3.6$  was also performed (Table 1). It should be noted that the enhancement of the activity of the complex due to the polymer was dependent on the DNA sequence. The activities of the heme( $\text{Fe}^{3+}$ )-6mer, heme( $\text{Fe}^{3+}$ )-6mer/p, heme( $\text{Fe}^{3+}$ )-6mer/T, and heme( $\text{Fe}^{3+}$ )-6mer/A complexes increased by factors of  $\sim 3$ ,  $\sim 18$ ,  $\sim 9$ , and  $\sim 1$ , respectively, upon the addition of the polymer (Table 1 and Fig. 4A). The heme( $\text{Fe}^{3+}$ )-6mer/p complex exhibited the greatest enhancement in the catalytic activity with the addition of PLL-*g*-Dex. In contrast, the activity of the

**Table 1.** Heme(Fe<sup>3+</sup>) Binding Constants [ $K_a$  ( $\mu\text{M}^{-1}$ )] of the Heme-DNA Complexes and Initial Slopes [ $R_0$  ( $\mu\text{M min}^{-1}$ )] of the Time Evolution of the 570-nm Absorbance Due to Resorufin Produced via Oxidation of Amplex Red in the Presence of the Heme-DNA Complexes without and with PLL-g-Dex.

Complex	$K_a^a$ ( $\mu\text{M}^{-1}$ )	$R_0^b$ ( $\mu\text{M min}^{-1}$ )	
			W / PLL-g-Dex <sup>c</sup>
Heme-6mer	$6.5 \pm 0.7^d$	$0.94 \pm 0.1^e$ ( $0.54 \pm 0.1$ ) <sup>g</sup>	$2.93 \pm 0.3$ ( $\sim 3$ ) <sup>f</sup>
Heme-6mer/p	$1.7 \pm 0.4$	$0.61 \pm 0.1$	$11.2 \pm 1.1$ ( $\sim 18$ ) <sup>f</sup>
Heme-6mer/T	$0.31 \pm 0.04^h$	$0.50 \pm 0.05^h$	$4.78 \pm 0.1$ ( $\sim 9$ ) <sup>f</sup>
Heme-6mer/A	$0.92 \pm 0.05^h$	$4.52 \pm 0.45^h$	$5.28 \pm 0.5$ ( $\sim 1$ ) <sup>f</sup>
Heme-18mer	$1.6 \pm 0.1^i$	$0.57 \pm 0.06^i$	$1.00 \pm 0.10$ ( $\sim 2$ ) <sup>f</sup>

<sup>a</sup> Measured in 300 mM KCl and 50 mM Potassium Phosphate Buffer at pH 6.80 and 25 °C.

<sup>b</sup> Measured at pH 6.80 and 25 °C.

<sup>c</sup> In the presence of PLL-g-Dex at  $N/P = 3.6$ .

<sup>d</sup> Measured as shown in Fig. S2.

<sup>e</sup> Obtained from ref. 16.

<sup>f</sup> The numbers in parentheses indicate the enhancement factors of the  $R_0$ s due to the addition of the polymer.

<sup>g</sup>  $\sim 100\%$   $\text{H}_2\text{O}$  was used as a solvent to evaluate deuterium kinetic isotope effects. The deuterium kinetic isotope effect (KIE (=  $R_0(^1\text{H})/R_0(^2\text{H})$ )) was determined to be 1.7.

<sup>h</sup> Obtained from ref. 19.

<sup>i</sup> Obtained from ref. 17.

heme(Fe<sup>3+</sup>)-6mer/A complex was not largely affected by the polymer, although it was the highest among those of the complexes in the absence of the polymer. Finally, the activity of heme(Fe<sup>3+</sup>) was not affected at all by the addition of the polymer (Fig. 4B), indicating that PLL-g-Dex cannot act as a cocatalyst for free heme(Fe<sup>3+</sup>). In addition, the activity of heme(Fe<sup>3+</sup>)-18mer complex increased by a factor of  $\sim 2$  upon the addition of the polymer (Table 1 and Fig. S6), indicating that the polymer acts as a cocatalyst for the peroxidase-mimicking complex between heme and an all parallel-stranded monomeric G-quadruplex DNA. Finally, the  $R_0$ s of the heme(Fe<sup>3+</sup>)-6mer and heme(Fe<sup>3+</sup>)-6mer/T complexes were not affected by the addition of dextran in amount equal to the weight of the dextran moiety of PLL-g-Dex at  $N/P = 3.6$  (Fig. S7), indicating that the hydroxy groups in dextran moieties of PLL-g-Dex is not involved in the enhancement of the catalytic activity of the complex. Finally, the TOF values of 1.9 and 5.9  $\text{min}^{-1}$  were obtained for the heme(Fe<sup>3+</sup>)-6mer complex in the absence and presence of PLL-g-Dex at  $N/P = 3.6$ , respectively (Fig. S8), indicating that the catalytic efficiency is fairly affected by the protonated and cationic polymer.<sup>58</sup>

### ESR characterization of Compound I

The peroxidase catalytic cycle of the heme(Fe<sup>3+</sup>)-DNA complex proceeds through the iron(IV)oxo porphyrin  $\pi$ -cation radical

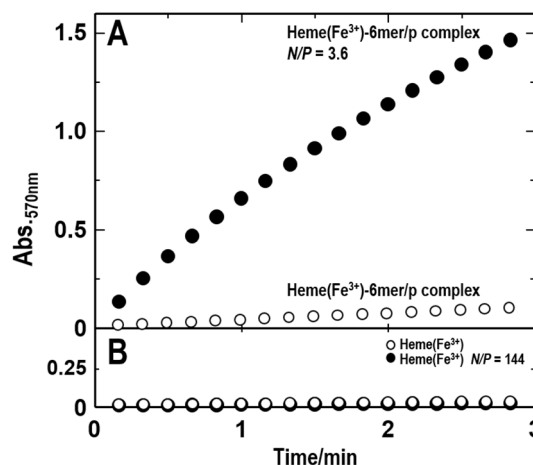


**Fig. 4** Time-evolution of 570-nm absorbance due to Resorufin produced on the oxidation of Amplex Red by the heme(Fe<sup>3+</sup>)-6mer/p complex in the absence (o) and presence of PLL-g-Dex at  $N/P = 3.6$  (●) (A), and heme(Fe<sup>3+</sup>) in the absence (o) and presence of PLL-g-Dex at  $N/P = 144$  (●) (B). Samples comprised 0.5  $\mu\text{M}$  heme(Fe<sup>3+</sup>), 20  $\mu\text{M}$  6mer/p (only for the heme(Fe<sup>3+</sup>)-6mer/p complex sample), 50  $\mu\text{M}$  Amplex Red, and 200  $\mu\text{M}$   $\text{H}_2\text{O}_2$ , in 50 mM  $\text{K}^+$  phosphate buffer, pH 6.80, at 25 °C. In (A), initial slopes ( $R_0$ s) of  $0.61 \pm 0.1$  and  $11.2 \pm 1.1$   $\mu\text{M min}^{-1}$  were obtained for the heme-6mer/p complex in the absence and presence of the polymer, respectively. In contrast, the  $R_0$  of heme(Fe<sup>3+</sup>), i.e.,  $0.15 \pm 0.01$   $\mu\text{M min}^{-1}$ ,<sup>16</sup> was unaffected by the addition of the polymer.

intermediate known as Compound I as a responsible species for the oxidation reaction.<sup>18</sup> The effect of PLL-g-Dex on the formation of Compound I in the catalytic cycle of the heme(Fe<sup>3+</sup>)-DNA complex was investigated by ESR measurement at liquid He temperature (Fig. 6). The ESR spectra of the heme(Fe<sup>3+</sup>)-6mer/p and heme(Fe<sup>3+</sup>)-6mer complexes in the presence of the polymer were similar to each other in terms of the axial signals with  $g_{\perp} = 5.94$  and  $g_{\parallel} = 2.00$ , and a rhombic high-spin type signal with  $g = 6.33$  (Figs. 6A and C). The spectra of samples prepared by freezing mixtures of the complex ([heme(Fe<sup>3+</sup>)-6mer/p complex] or [heme(Fe<sup>3+</sup>)-6mer complex] = 0.1 mM), in the presence of PLL-g-Dex at  $N/P = 3.75$ , and [ $\text{H}_2\text{O}_2$ ] = 15 mM in phosphate buffer solutions, pH 6.80 (the interval between mixing and freezing being  $\sim 3$  s), exhibited convex peaks at  $g = \sim 2$  (Figs. 6B and D). On the basis of the literature to report the ESR spectrum of Compound I derived from HRP,<sup>59,60</sup> the signal at  $g = \sim 2$  was assigned to that of Compound I derived from the heme-DNAzymes. In addition, a signal at  $g = \sim 6$ , derived from an unreacted ferric high-spin species, and one at  $g = 4.27$  due to degraded heme<sup>61</sup> were observed, and the rhombic high-spin type signal at  $g = \sim 6.3$  was observed as a shoulder of a peak at  $g = \sim 5.9$  in the spectra of the complexes (Figs. 6B and D). Furthermore, the intensity ratio between the signals at  $g = \sim 2$  and  $g = \sim 6$  ( $I_{(g=2)}/I_{(g=6)}$ ) was obtained through double integration of the spectra (Fig. 7) and was used as a quantitative measure for Compound I generated in the reaction mixtures. The  $I_{(g=2)}/I_{(g=6)}$  values of 0.0047 and 0.0114 were obtained for the spectra of the heme(Fe<sup>3+</sup>)-6mer and heme(Fe<sup>3+</sup>)-6mer/p complexes in the presence of PLL-g-Dex at  $N/P = 3.75$ , respectively, and the value of 0.0034 was obtained for the spectrum of the heme(Fe<sup>3+</sup>)-6mer one in the absence of

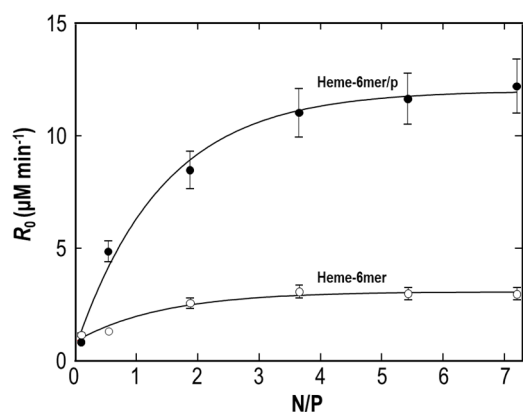


**Fig. 5** Plots of the  $R_0$ s against the  $N/P$  for the heme( $\text{Fe}^{3+}$ )-6mer (o) and heme( $\text{Fe}^{3+}$ )-6mer/p complexes (●). The  $R_0$ s of the complexes increased with increasing  $N/P$  and almost reached plateaus at  $N/P > 3.6$ .

the polymer (Fig. 7). The order of  $I_{(g-2)}/I_{(g-6)}$  for the complexes, i.e., heme( $\text{Fe}^{3+}$ )-6mer complex < heme( $\text{Fe}^{3+}$ )-6mer complex with the polymer < heme( $\text{Fe}^{3+}$ )-6mer/p complex with the polymer, is identical to that of increasing  $R_0$  (Table 1).

## DISCUSSION

### Characterization of an interpolyelectrolyte complex between the heme-6mer complex and PLL-g-Dex

The effects of the PLL-g-Dex binding on structural properties of the heme-6mer complex could be elucidated through the polymer concentration-dependent appearance of the  $^1\text{H}$  NMR spectrum of the CO adduct of the complex (Figs. 3B-B<sup>''</sup>). Shifts of the resolved G4<sub>C</sub>-G6<sub>C</sub>, heme *meso*, and  $\Delta_{\text{H}_2\text{O}}$  proton signals of the complex were almost independent of the addition of the polymer, indicating that the interaction between heme and DNA in the complex as well as the structure of the G-quadruplex DNA are not largely affected by the binding of the polymer. The broadening of the resolved NMR signals with increasing polymer concentration, as seen in Figs. 3B-B<sup>''</sup>, can be explained in terms of an increase in the apparent molecular weight of the complex through the polymer binding, which results in a slowdown of the molecular motion, and hence a shortening of spin-spin relaxation time  $T_2$ , confirming the formation of a stable interpolyelectrolyte complex. In addition, peaks x-z, i.e., G4<sub>D</sub>-G6<sub>D</sub> proton signals, appeared and their intensities increased with increasing polymer concentration (Figs. 3B-B<sup>''</sup>). These results indicate that the dimerization of 6mer<sup>52</sup> (Fig. S4) takes place concomitantly with detachment of heme from the complex in the presence of the polymer, possibly due to electrostatic interaction between propionate side chains of heme and positive charges of the polymer (Figs. 1A and E, respectively). Detached heme( $\text{Fe}^{2+}$ ) is thought to be spontaneously and rapidly oxidized to become a high-spin heme( $\text{Fe}^{3+}$ ) of which NMR signals are observed well outside of the spectral region depicted in Fig. 3.<sup>62</sup>

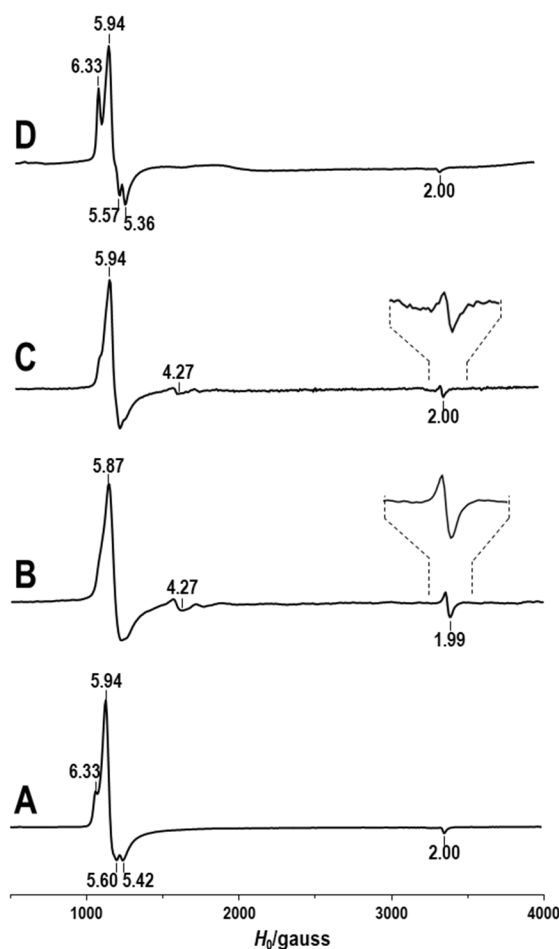


**Fig. 6** ESR spectra of the heme( $\text{Fe}^{3+}$ )-6mer/p (A) and heme( $\text{Fe}^{3+}$ )-6mer complexes (C) in the presence of PLL-g-Dex at  $N/P = 3.75$  and the heme( $\text{Fe}^{3+}$ )-6mer/p (B) and heme( $\text{Fe}^{3+}$ )-6mer ones (D) in the presence of PLL-g-Dex at  $N/P = 3.75$  after addition of a 150-fold stoichiometric excess of  $\text{H}_2\text{O}_2$ . Spectra were recorded at 5 K. In (B) and (C), the Y-gains of Compound I signals near  $g = 2$  are expanded by a factor of  $\sim 2.5$ .

The detachment of heme from the heme-DNA complex due to the polymer leads to a decrease in the concentration of the active complex, which in turn results in a decrease in the peroxidase activity of the complex. However, since the peroxidase assay of the complex was performed in the presence of a large excess of G-quadruplex DNA, i.e.,  $[\text{heme}(\text{Fe}^{3+})] = 0.5 \mu\text{M}$  and  $[\text{G-quadruplex DNA}] = 20 \mu\text{M}$ , the effect of the heme detachment due to the polymer on the activity, i.e., the  $R_0$ , of the complex, is thought to be rather limited, as manifested in the polymer concentration-dependent activities of the complexes shown in Fig. 5.

### Effect of PLL-g-Dex on peroxidase activity of the heme-DNA complex

The enhancement of the catalytic activity of the heme( $\text{Fe}^{3+}$ )-DNA complex by PLL-g-Dex (Fig. 4A) clearly indicated that, within the interpolyelectrolyte complex between the heme( $\text{Fe}^{3+}$ )-DNA complex and the polymer, protonated amino groups ( $-\text{NH}_3^+$



and  $\text{-NH}_2^+$ ) of the polymer can be located close enough to an  $\text{Fe}^{3+}$ -bound hydroperoxo ( $\text{Fe}^{3+}\text{-OOH}$ ) moiety to act as general acid catalysts, like the Arg38 side chain in HRP (Scheme 1B), to promote the O-O bond heterolysis for a  $\text{Fe}^{3+}\text{-OOH}$  intermediate toward the formation of Compound I (Scheme 1A). The oxidative conversion of Amplex Red to Resorufin proceeds through a proton-coupled electron transfer reaction.<sup>57</sup> The oxidation potential of Amplex Red in aqueous solution was not largely affected by the addition of PLL-g-Dex (Fig. S5). In addition, the  $\text{pK}_a$  of Amplex Red, i.e.,  $\text{pK}_a \sim 9$ ,<sup>57</sup> has been reported, indicating that the Amplex Red is not deprotonated to possess two phenolic protons in the phosphate buffer at pH 6.80 and in the presence of the acidic polymer having protonated amino groups. Thus, the oxidation potential of Amplex Red was not affected by the addition of the protonated polymer, suggesting that the enhancement of the oxidation reaction is due to the electron transfer from the substrate to the Compound I. The KIE value of 1.7 obtained for the oxidation reaction using the heme-6mer complex (Table 1) indicates that the hydrogen atom transfer from one of the phenolic hydroxyl groups of Amplex Red to Compound I is involved in the rate-determining step.<sup>63</sup> Consequently, it should be reasonable to propose that the enhancement of the Compound I generation by the polymer results in an increase in the  $R_0$ .

The local heme environment in the interpolyelectrolyte complex can be inferred from the enhancement of the activity of the heme( $\text{Fe}^{3+}$ )-DNA complex by PLL-g-Dex (Table 1). In the interpolyelectrolyte complex between the heme( $\text{Fe}^{3+}$ )-6mer/p complex and the polymer, due to favorable electrostatic interactions of the 3'-terminal phosphate groups of the DNA with the polymer, the interpolyelectrolyte complex is stabilized, and protonated amino groups of the polymer become located in close proximity to the heme to promote the formation of Compound I as general acid catalysts, leading to  $\sim 18$ -fold enhancement of the activity of the heme( $\text{Fe}^{3+}$ )-6mer/p complex by the polymer (Table 1). Thus, the enhancement of the peroxidase activity of the heme( $\text{Fe}^{3+}$ )-DNA complex by PLL-g-Dex was found to be affected by the negative charge density of the terminal phosphate group of 6mer/p in the proximity of the heme binding site of the complex, causing strong binding of the cationic polymer (Fig. 8A). Similarly, in an interpolyelectrolyte complex between the heme( $\text{Fe}^{3+}$ )-6mer/T complex and the polymer, positive charges of the polymer interact electrostatically with the phosphate groups in the phosphodiester bond at the G6T7 step of 6mer/T, and hence protonated amino groups of the polymer become located close enough to act as general acid catalysts, as manifested in the  $\sim 9$ -fold enhancement of the activity of the complex by the polymer (Table 1). Therefore, although heme( $\text{Fe}^{3+}$ ) is located between the G6 G-quartet and T7 bases of 6mer/T in the heme( $\text{Fe}^{3+}$ )-6mer/T complex,<sup>15</sup> it is proposed that the accessibility of the substrate, i.e., Amplex Red, to the  $\text{Fe}^{4+}=\text{O}$  moiety in Compound I (Scheme 1A) is not largely restricted by steric hindrance around the heme( $\text{Fe}^{3+}$ ), due to the nearby T7 bases. On the other hand, in the case of the heme( $\text{Fe}^{3+}$ )-6mer/A complex, the A7 base itself acts as a general base catalyst to promote the formation of Compound I through its proton-accepting character as to deprotonated  $\text{Fe}^{3+}$ -bound  $\text{H}_2\text{O}_2$  (Fig.

8B),<sup>17</sup> and hence the activity of the complex was not further enhanced by the addition of the polymer to the complex. Finally, due to the absence of 3'-terminal phosphate groups in the 6mer, protonated amino groups of the polymer in an

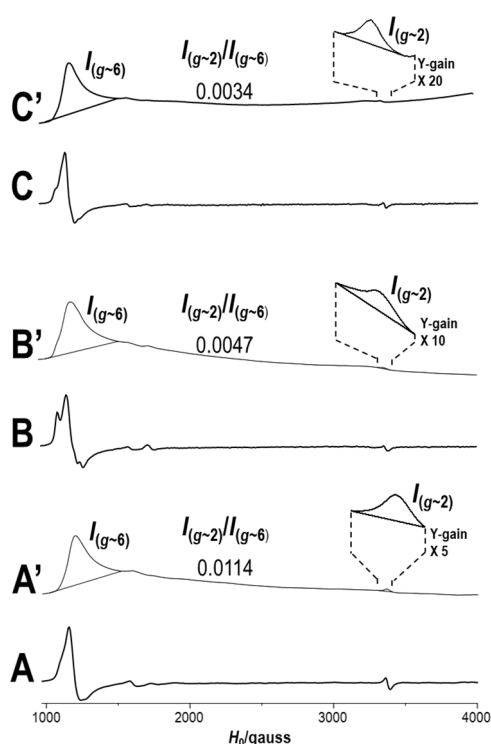


**Fig. 7** Analysis of ESR signal intensity through double integration. The heme( $\text{Fe}^{3+}$ )-6mer/p complex in the presence of PLL-*g*-Dex at  $N/P = 3.75$  (A), and the heme( $\text{Fe}^{3+}$ )-6mer one in the presence of PLL-*g*-Dex at  $N/P = 3.75$  (B) and absence of the polymer (C). The results from double integration of spectra A, B, and C are shown in A', B', and C', respectively. The spectra of samples were obtained by freezing mixtures of the complex ([heme( $\text{Fe}^{3+}$ )-6mer complex] or [heme( $\text{Fe}^{3+}$ )-6mer/p complex] = 0.1 mM), in the presence of PLL-*g*-Dex at  $N/P = 3.75$ , and  $[\text{H}_2\text{O}_2] = 15$  mM in phosphate buffer solutions, pH 6.80 (the interval between mixing and freezing being  $\sim 3$  s). The ratio of the intensity between the signals at  $g \sim 2$  and  $g \sim 6$  ( $I_{(g=2)}/I_{(g=6)}$ ) was used as a quantitative measure for Compound I generated in the reaction mixture.  $I_{(g=2)}/I_{(g=6)}$  values of 0.0114 and 0.0047 were obtained from the spectra of the heme( $\text{Fe}^{3+}$ )-6mer/p and heme( $\text{Fe}^{3+}$ )-6mer complexes in the presence of the polymer, respectively, and one of 0.0034 for the spectrum of the heme( $\text{Fe}^{3+}$ )-6mer one in the absence of the polymer. Spectrum C was taken from ref. 18.

interpolyelectrolyte complex between the heme( $\text{Fe}^{3+}$ )-6mer complex and the polymer might not be kept in close proximity to the heme( $\text{Fe}^{3+}$ ) in the complex, and hence their optimal general acid catalytic action would not be effective, as reflected in the  $\sim 3$ -fold enhancement of the activity of the complex by the polymer (Table 1). In addition, the importance of negative charge density in the vicinity of the heme is exemplified by the lack of enhancing effect of the polymer on the free heme as demonstrated in Fig. 4B; the electrostatic interaction between negatively-charged propionate side chains of free heme and positively-charged protonated amino groups of the polymer is not strong enough to force the protonated amino groups to be located in close proximity of the heme to promote the formation of Compound I.

The enhancement of the catalytic activity of the heme( $\text{Fe}^{3+}$ )-DNA complex by PLL-*g*-Dex could be reasonably explained in terms of the effect of the polymer on the formation of Compound I in the catalytic cycle of the heme-DNA complex, characterized

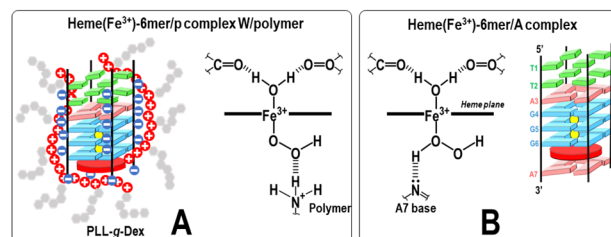


**Fig. 8** Schematic illustration of general acid catalysis of a protonated amino group ( $-\text{NH}_3^+$ ) of PLL-*g*-Dex in an interpolyelectrolyte complex between the heme-6mer/p complex and polymers (A), and general base catalysis of the A7 base of the heme-6mer/A complex (B). Due to the 3'-terminal phosphate groups, the interpolyelectrolyte complex is stabilized and  $-\text{NH}_3^+$  located in close proximity to the heme promotes the formation of Compound I as a general acid catalyst (A), and the A7 base acts as a general base catalyst to promote the formation of Compound I through its proton-accepting character as to deprotonated  $\text{Fe}^{3+}$ -bound  $\text{H}_2\text{O}_2$  (B).

through analysis of ESR signal intensity estimated using double integration. In the ESR spectra of the complexes, the intensity of the signal at  $g \sim 2$  due to Compound I, relative to that of the signal at  $g \sim 6$  due to ferric high-spin species,  $I_{(g=2)}/I_{(g=6)}$ , was affected by the addition of PLL-*g*-Dex (Figs. 6 and 7). The  $I_{(g=2)}/I_{(g=6)}$  of the heme( $\text{Fe}^{3+}$ )-6mer complex increased by a factor of 1.4 on the addition of the polymer, indicating that Compound I generation in the catalytic cycle of the complex is enhanced by the polymer. In addition, in the presence of the polymer, the  $I_{(g=2)}/I_{(g=6)}$  of the heme( $\text{Fe}^{3+}$ )-6mer/p complex was larger by a factor of 2.4 compared with that of the heme( $\text{Fe}^{3+}$ )-6mer one, indicating that the degree of enhancement of Compound I generation by the polymer is affected by the local heme environment of the complex. Furthermore, the  $I_{(g=2)}/I_{(g=6)}$  values of the complexes correlated well with their  $R_{0s}$  (Table 1). These results unequivocally indicated that PLL-*g*-Dex could be a cocatalyst for peroxidase-mimicking heme-DNAzymes by forming an appropriate micro-environment and acting as a general acid catalyst. The greater enhancement of Compound I generation in the catalytic cycle of the heme( $\text{Fe}^{3+}$ )-6mer/p complex by the polymer can be explained in terms of the electrostatic environment around the heme in the complex, as described above. In the interpolyelectrolyte complex between the heme( $\text{Fe}^{3+}$ )-6mer/p complex and PLL-*g*-Dex, the 3'-terminal phosphate groups of the DNA, in addition to the phosphate groups in the phosphodiester bonds, contribute to not only improvement of the stability of the interpolyelectrolyte complex, but also arranging protonated amino groups of the polymer in the close proximity to the heme to provide general acid catalysts for the acceleration of Compound I formation. These findings pave a way for designing novel catalytic interpolyelectrolyte complexes composed of the heme-DNAzyme and cationic polymers.

## Conclusions

In this study, we have demonstrated that a cationic copolymer possessing protonated amino groups can be used as a cocatalyst

to facilitate the formation of Compound I as a reactive species for a peroxidase-mimicking heme-DNAzyme. The cationic polymer binds to the anionic DNAzyme to form an interpolyelectrolyte complex, and its protonated amino groups facilitate heterolytic O-O bond cleavage of an Fe<sup>3+</sup>-hydroperoxy species to generate the iron(IV)oxo porphyrin  $\pi$ -cation radical intermediate known as Compound I; this enhancement is reminiscent of the general acid catalysis by the positively-charged Arg38 residue in HRP. The ability of the polymer as the general acid cocatalyst was found to be affected by the local heme environment of the heme-DNAzyme, such as steric hindrance and the local negative charge density around the heme moiety. These findings provide a novel guideline as to the molecular design of heme-DNAzymes for enhancing the catalytic activity in oxidation reactions.

### Conflicts of interest

There are no conflicts to declare.

### Acknowledgements

The acknowledgements come at the end of an article after the conclusions and before the notes and references. This work was financially supported by JSPS KAKENHI (Nos. 19H02824 and 20H05496 to Y.Y. and 19H04560 to T. K.), the Center of Innovation Program (JPMJCE1305) of the Japan Science and Technology Agency, the cooperative research program of the “Network Joint Research Center for Materials and Devices” (to A. M.), a Grant-in-Aid for Transformative Research Areas “Molecular Cybernetics” (20A40, to N.S.) from MEXT, and the Research Program on Emerging and Re-emerging Infectious Diseases (JP 19fk0108152h0001) of AMED (to A. M.).

### References and notes

- B. Chance, R. W. Estabrook and T. Yonetani, eds. *Hemes and Hemoproteins*, Academic Press: New York, NY, 1966.
- P. Travascio, Y. Li and D. Sen, *Chem. Biol.*, 1998, **5**, 505–517.
- P. Travascio, A. J. Bennet, D. Y. Wang and D. Sen, *Chem. Biol.*, 1999, **6**, 779–787.
- P. Travascio, P. K. Witting, A. G. Mauk and D. Sen, *J. Am. Chem. Soc.*, 2001, **123**, 1337–1348.
- P. Travascio, D. Sen and A. J. Bennet, *Can. J. Chem.*, 2006, **84**, 613–619.
- L. C. Poon, S. P. Methot, W. Morabi-Pazooki, F. Pio, A. J. Bennet and D. Sen, *J. Am. Chem. Soc.*, 2011, **133**, 1877–1884.
- D. Sen and C. R. Geyer, *Curr. Opin. Chem. Biol.*, 1998, **2**, 680–687.
- D. Sen and L. C. Poon, *Crit. Rev. Biochem. Mol. Biol.*, 2011, **46**, 478–492.
- N. Shumayrikh and D. Sen, *Methods Mol. Biol.*, 2019, **2035**, 357–368.
- T. Mikuma, T. Ohyama, N. Terui, Y. Yamamoto and H. Hori, *Chem. Commun.*, 2003, 1708–1709.
- K. Saito, H. Tai, M. Fukaya, T. Shibata, R. Nishimura, S. Neya and Y. Yamamoto, *J. Biol. Inorg. Chem.*, 2012, **17**, 437–445.
- K. Saito, H. Tai, H. Hemmi, N. Kobayashi and Y. Yamamoto, *Inorg. Chem.*, 2012, **51**, 8168–8176.
- Y. Suzuki, H. Tai, K. Saito, Shibata, M. Kinoshita, A. Suzuki and Y. Yamamoto, *J. Porphyrins Phthalocyanines*, 2014, **18**, 741–751.
- Y. Yamamoto, M. Kinoshita, Y. Katahira, H. Shimizu, Y. Di, T. Shibata, H. Tai, A. Suzuki and S. Neya, *Biochemistry*, 2015, **54**, 7168–7177.
- H. Shimizu, H. Tai, K. Saito, T. Shibata, M. Kinoshita and Y. Yamamoto, *Bull. Chem. Soc. Jpn.*, 2015, **88**, 644–652.
- R. Shinomiya, Y. Katahira, H. Araki, T. Shibata, A. Momotake, S. Yanagisawa, T. Ogura, A. Suzuki, S. Neya and Y. Yamamoto, *Biochemistry*, 2018, **57**, 5930–5937.
- Y. Yamamoto, H. Araki, R. Shinomiya, K. Hayasaka, Y. Nakayama, K. Ochi, T. Shibata, A. Momotake, T. Ohyama, M. Hagihara and H. Hemmi, *Biochemistry*, 2018, **57**, 5938–5948.
- R. Shinomiya, H. Araki, A. Momotake, H. Kotani, T. Kojima and Y. Yamamoto, *Bull. Chem. Soc. Jpn.*, 2018, **92**, 1729–1736.
- C. Okamoto, A. Momotake and Y. Yamamoto, *J. Inorg. Biochem.*, 2021, **216**, 111336.
- N. Shumayrikh, Y. C. Huang and D. Sen, *Nucleic Acids Res.*, 2015, **43**, 4191–4201.
- D.M. Kong, *Methods*, 2013, **64**, 199–204.
- L. Zhu, C. Li, Z. Zhu, D. Liu, Y. Zou, C. Wang, H. Fu and C. J. Yang, *Anal. Chem.*, 2012, **84**, 8383–8390.
- J. Chen, Y. Guo, J. Zhou and H. Ju, *Chem.-A Eur. J.*, 2017, **23**, 4210–4215.
- W. Li, Y. Li, Z. Liu, B. Lin, H. Yi, F. Xu, Z. Nie and S. Yao, *Nucleic Acids Res.*, 2016, **44**, 7373–7384.
- T. Chang, H. Gong, P. Ding, X. Liu, W. Li, T. Bing, Z. Cao and D. Shangguan, *Chem.-A Eur. J.*, 2016, **22**, 4015–4021.
- A. Virgilio, V. Esposito, P. Lejault, D. Monchaud and A. Galeone, *Int. J. Biol. Macromol.*, 2020, **151**, 976–983.
- S. Nakayama and H. O. Sintim, *J. Am. Chem. Soc.*, 2001, **123**, 11838–11847.
- S. Nakayama and H. O. Sintim, *Compounds. Mol. BioSyst.*, 2010, **17**, 14475–14484.
- S. Nakayama, J. Wang and H. O. Sintim, *Chem.-Eur. J.*, 2011, **17**, 5691–51698.
- S. Nakayama and H. O. Sintim, *Anal. Chim. Acta.*, 2011, **136**, 1569–1572.
- C. Qi, N. Zhang, J. Yan, X. Liu, T. Bing, H. Mei and D. Shangguan, *RSC Adv.*, 2014, **4**, 1441–1448.
- E. Golub, H. B. Albada, W.-C. Liao, Y. Biniuri and I. Willer, *J. Am. Chem. Soc.*, 2016, **138**, 164–172.
- Q. Liu, H. Wang, X. Shi, Z.-G. Wang and B. Ding, *ACS Nano*, 2017, **11**, 7251–7258.
- Z.-G. Wang, Y. Li, H. Wang, K. Wan, Q. Liu, X. Shi and B. Ding, *Chem.-A Eur. J.*, 2019, **25**, 12576–12582.
- J. Chen, J. Wang, S. C. C. van der Lubbe, M. Cheng, D. Qiu, D. Monchaud, J. L. Mergny, F. G. Guerra, H. Ju and J. Zhou, *CCC Chem.*, 2020, **2**, 2183–2193.
- J. H. Dawson and M. Sono, *Chem. Rev.*, 1987, **87**, 1255–1276.
- M. Sono, M. P. Roach, E. D. Coulter and J. H. Dawson, *Chem. Rev.*, 1996, **96**, 2841–2888.
- J. H. Dawson, *Science*, 1988, **240**, 433–439.
- J. N. Rodríguez-López, D. J. Lowe, J. Hernández-Ruiz, A. N. Hiner, F. García-Cánovas and R. N. Thorneley, *J. Am. Chem. Soc.*, 2001, **123**, 11838–11847.
- M. Gajhede, D. J. Schuller, A. Henriksen, A. T. Smith and T. J. Poulos, *Nat. Struct. Biol.*, 1997, **4**, 1032–1038.

- 41 M. Ortmayer, K. Fisher, J. Basran, E. M. Wolde-Michael, D. J. Heyes, C. Levy, S. L. Lovelock, J. L. R. Anderson, E. L. Raven, S. Hay, S. E. J. Rigby and A. P. Green, *Nat. Struct. Biol.*, 2020, **4**, 1032-1038.
- 42 D. Sen and W. Gilbert, *Nature*, 1988, **334**, 364-366.
- 43 A. Maruyama, M. Katoh, T. Ishihara and T. Akaike, *Bioconjugate Chem.*, 1997, **8**, 3-6.
- 44 Y. Sato, Y. Kobayashi, T. Kamiya, H. Watanabe, T. Akaike, K. Yoshikawa and A. Maruyama, *Biomaterials*, 2005, **26**, 703-711.
- 45 L. Wu, N. Shimada, A. Kano and A. Maruyama, *Soft Matter*, 2008, **4**, 744-747.
- 46 R. Moriyama, N. Shimada, A. Kano and A. Maruyama, *Biomaterials*, 2011, **32**, 2351-2358.
- 47 R. Moriyama, N. Shimada, A. Kano and A. Maruyama, *Biomaterials*, 2011, **32**, 7671-7676.
- 48 J. Du, L. Wu, N. Shimada, A. Kano and A. Maruyama, *Chem. Commun.*, 2013, **49**, 475-477.
- 49 N. Yamaguchi, Y. Zouzumi, N. Shimada, S. Nakano, N. Sugimoto, A. Maruyama and D. Miyoshi, *Chem. Commun.*, 2016, **52**, 7446-7449.
- 50 H. Sato, N. Shimada, T. Masuda and A. Maruyama, *Biomacromolecules*, 2018, **19**, 2082-2088.
- 51 P. Thaplyal and P. C. Bevilacqua, *Methods Enzymol.*, 2014, **549**, 189-219.
- 52 R. Del Villar-Guerra, R. D. Gray and J. B. Chaires, *Curr. Protoc. Nucleic Acid Chem.*, 2017, **2**, 1-17.
- 53 Y. Wang, K. Hamasaki and R. R. Rando, *Biochemistry*, 1997, **36**, 768-779.
- 54 G. N. La Mar, D. L. Budd, D. B. Viscio, K. M. Smith and K. C. Langry, *Proc. Natl. Acad. Sci. U. S. A.*, 1978, **75**, 5755-5759.
- 55 G. N. La Mar, Y. Yamamoto, T. Jue, K. M. Smith and R. K. Pandey, *Biochemistry*, 1985, **24**, 3826-3831.
- 56 Y. Kato, T. Ohyama, H. Mita and Y. Yamamoto, *J. Am. Chem. Soc.*, 2005, **127**, 9980-9981.
- 57 D. Dębski, R. Smulik, J. Zielonka, B. Michałowski, M. Jakubowska, K. Dębowska, J. Adamus, A. Marcinek, B. Kalyanaraman and A. Sikora, *Free Radc. Biol. Med.*, 2016, **95**, 323-332.
- 58 We determined the TOF of HRP to be  $1.1 \times 10^4 \text{ min}^{-1}$  under the same conditions except the concentration of the catalyst,  $[\text{HRP}] = 1 \text{ nM}$  (Fig. S9). The value was considerably larger than that of the heme( $\text{Fe}^{3+}$ )-6mer complex, i.e.,  $1.9 \text{ min}^{-1}$  (Fig. S8).
- 59 H. Fujii, T. Yoshimura and H. Kamada, *Inorg. Chem.*, 1996, **35**, 2373-2377.
- 60 A. Takahashi, T. Kurahashi and H. Fujii, *Inorg. Chem.*, 2009, **48**, 2614-2625.
- 61 M. Tanaka, K. Ishimori, M. Mukai, T. Kitagawa and I. Morishima, *Biochemistry*, 1997, **36**, 9889-9898.
- 62 D. L. Budd, G. N. La Mar, K. C. Langry, K. M. Smith and R. Nayyir-Mazhir, *J. Am. Chem. Soc.*, 1979, **101**, 6091-6096.
- 63 S. Ohzu, T. Ishizuka, H. Kotani and T. Kojima, *Chem. Commun.*, 2014, **50**, 15018-15021.